Synthesis and Optimization of Trimethylolpropane-Based Biolubricant from A Blend of Crude Soybean, Fish, and Waste Peanut Oils

*Aliru Olajide Mustapha, Muhammed Hatim Garuba, and Halimat Feyishayo Olasode,

https://doi.org/10.33003/frscs-2025-0402/07

Accepted: 11th June, 2025
Published: 05th July, 2025

1. Department of Chemistry and Industrial Chemistry, Faculty of Pure and Applied Sciences, Kwara State University Malete, PMB 1530, Ilorin, Kwara State, Nigeria.

*<u>*Corresponding Author:</u>*
Aliru Olajide Mustapha
aliru.mustapha@kwasu.edu.ng

FRsCS Vol. 4 No. 2 (2025)
Official Journal of Dept. of Chemistry, Federal University of Dutsin-Ma, Katsina State.
http://rscs.fudutsinma.edu.ng

ISSN (Online): 2705-2362
ISSN (Print): 2705-2354

Abstract

The study aimed to create a trimethylolpropane-based biolubricant from crude edible and waste cooking oils to reduce greenhouse gas emissions and global warming. The biolubricant was produced through two-steps esterification and transesterification reactions using trimethylolpropane (TMP) in the presence of potassium hydroxide and methanol. A Box-Behnken Design (BBD)-based response surface methodology was utilized to optimize the reaction conditions, including blend oil methyl ester (BOME) to TMP molar ratio (3:1–7:1 wt%), temperature (60–100 ˚C), and reaction time (60–120 min), in 17 experimental procedures to achieve enhanced triester yield. The quadratic model was found to adequately predict the test yield, with an R^2 value of 0.9054. An optimum yield of 91.097% was suggested at a molar ratio of 6.5:1 wt%, a temperature of 61.1 ˚C, and a reaction time of 60.8 min, which correlates with the experimentally mean value of 90.977% with a 0.13% difference. The physicochemical properties of the blended oil triester (BTE) showed viscosity of 72.7 and 11.8 mPa/s at 40 and 100 ˚C, a viscosity index of 136, a flash point of 205 ˚C, and a pour point of -2.5 ˚C.

Keywords: Optimization, transesterification, biolubricant, blend, BBD-RSM, trimethylolpropane.

Introduction

The Fossil fuels have played a vital role in addressing global energy demands for centuries. However, fossil resources are decreasing over the years due to the increasing energy demands resulting from industrialization and population expansion (Zayyanu et al., 2024). As a result, the use of fossil fuels is a major global issue since it poses a serious threat to the environment. These fuels are associated with the emission of greenhouse gases, which are the primary cause of climate change, flooding, drought, and the development of infectious diseases (Ejike et al., 2021). Lubricants are essential in industries, vehicles, and aircraft machinery, mainly to reduce frictional resistance (Alang et al., 2018). However, conventional lubricants are based on these fossil fuels and have severe environmental effects due to their non-biodegradability, toxicity, and non-renewability (Nkem & Nwakaudu, 2019). The current increased demand for energy, the rising cost of crude oil, greenhouse gas emissions that cause global warming, environmental pollution, lowbiodegradability, and the rapidly decreasing availability of fossil fuels are among the major concerns driving the search for alternative energy sources such as bio-based fuel and lubricants (Chaiendoo et al., 2025; Ejike et al., 2021).

Biolubricants offer numerous environmental, health, and performance benefits over petroleum-based lubricants. They are degradable, eco-friendly, and renewable, posing minimal risk to the environment or operators (Appiah *et al.,* 2021). However, they are not widely used commercially due to drawbacks like high pour point, low temperature, low thermal-oxidative stability, high initial cost per volume, and competition with food production (Ocholi *et al.,* 2018). These issues are attributed to the carbon-carbon double bond in the fatty acid chain and beta hydrogen on glycerol, which are prone to oxygen attack (Nkem & Nwakaudu, 2019).

Vegetable oils can be modified through various chemical processes, such as epoxidation, esterification, transesterification, hydrogenation, and estolide formation (Raof *et al.,* 2022). The esterification and transesterification process is the most common and widely used, as it involves substituting the glycerol backbone with a polyhydric alcohol like neopentylglycol (NPG), trimethylolpropane (TMP), pentaerythritol (PE), or dipentaerythritol (diPE) to form a synthetic ester. TMP is the most commonly used polyol ester due to its availability and affordability (Raof *et al*., 2022).

Over time, research has been conducted on novel feedstocks and chemical modification methods for improving vegetable oils and optimizing the chemical modification process. A variety of oleaginous plants, including sweet almond, *Jatropha curcas*, sesame, coconut, soybean, jojoba, rapeseed, palm, and sunflower oil, have been examined for their potential as lubricants (Mustapha *et al*., 2023; Thanaphorn *et al*., 2018). Furthermore, the use of waste cooking oil (WCO) for biolubricant synthesis is growing due to its accessibility and affordability compared to virgin oils (Bashiri *et al.,* 2021). WCO-based biolubricants have significantly improved characteristics such as flash point, viscosity index, and pour point compared to the ISO VG10 base oil standard, making it a sustainable and intelligent alternative to petroleum-based lubricants (Soufi *et al*., 2019). While substantial progress has been achieved in the synthesis and optimization of biolubricants derived from renewable sources, the majority of current research focuses on virgin oils or waste cooking oil as the only feedstock. However, the possibilities of developing a biolubricant from blends of crude and waste oils as feedstock while optimizing the reaction conditions to achieve a high yield remain understudied.

This study aims to use the transesterification reaction approach to create a TMP-based biolubricant with improved physicochemical properties from a blend of crude soybean, fish, and waste peanut oils while applying a Box-Behnken experimental design to statistically model, analyze, and optimize the reaction process to obtain a high yield. The reaction conditions (molar ratio, temperature, and reaction time) are optimized using response surface methodology (RSM) based on Box Behnken design (BBD) to estimate the effects of variables and their interactions. RSM is a flexible mathematical technique used in optimization, modelling, and experimental design, and has been applied to transesterification processes (Betiku *et al*., 2016). The fundamental methods involve fitting predictor functions to response variables and examining the properties of the fitted surface to determine the appropriate action (Shaba *et al*., 2018).

Materials and Methods

Materials

Samples including waste peanut oil (WPO), crude soybean oil (CSO), and crude fish oil (CFO), chemicals and reagents including methanol (99.5%), potassium hydroxide (85.0%), isopropyl alcohol (99.7%), sodium hydroxide (98.0%), sodium chloride (99.0%), sulphuric acid (95.0%), trimethylolpropane (98.0%), phenolphthalein indicator, activated charcoal, starch, and wij's reagent were all of analytical grade and were obtained from Sigma Aldrich (UK) and Teddington Middlesex, (UK). A Pour point analyzer (SETA–LEC Cloud and Pour Point Refrigerator), a Themometer, a multi-flash flash point tester (Model: 34000), a Brookfield® (Synchro-lectric Viscometer: RVT), a C5 bench-top centrifuge, and an analytical balance were also used in this study.

Methods

Preparations of Samples

The samples were collected from markets in Ilorin, Kwara State, Nigeria. After which, they were drained, filtered, washed, and decanted. Subsequently, the oils were pre-treated using a direct esterification process with methanol and sulphuric acid to reduce their free fatty acid (FFA) content and refined, including degumming, alkaline treatment, and bleaching treatment, using modified procedures as described by Mustapha *et al.* (2021).

Each mixture was made with 2.25 mL methanol and 0.05 mL (5 % w/w) sulphuric acid for each gram of free fatty acid in the oils of known FFA value, and was slowly added to the three oils separately. The resulting mixture was agitated for about one hour at 60-65 ºC and allowed to settle. The mixture formed two layers after settling (otherwise, 50 mL of warm distilled water was used to wash the mixture 3-4 times to encourage separation). These layers (aqueous layer and oil) were separated by decantation using a separating funnel. The fraction at the bottom of the funnel was then used for the new FFA level determination using the titrimetric method. The pre-treatment process was repeated when the FFA value was higher than 1 %.

The amount of methanol used was calculated using the equation:

$$N_M = \frac{2.25 \times \%\ \mathrm{FFA} \times W_o}{100} \qquad (1)$$

The amount of sulphuric acid used was calculated using the equation:

$$N_S = \frac{0.05 \times \mathrm{FFA} \times W_o}{100}, \qquad (2)$$

where N_M is the amount of methanol, N_S is the amount of concentrated sulphuric acid, % FFA is the percentage free fatty acid in the sample, and W_o is the weight of the oil sample.

Refinement of the WPO, CSO, and CFO

Refinement of the oil is an important phase in biolubricant production for removing impurities such as phosphorus compounds before efficient trans-esterification. The refining processes include: degumming, alkaline treatment (neutralization), and bleaching treatment were carried out (Mustapha *et al.,* 2021).

(a) Degumming Treatment

A 100 mL of the oils was separately mixed with 20 mL of the aqueous 300μg/mL NaCl (aq) solution. The mixture was continuously agitated at 60 ºC for 1hour on a hot plate with constant stirring. The insoluble phosphatides obtained were separated using a C5 bench-top centrifuge at 1000 rpm for about 30 minutes. The colloidal mixture formed was then removed from the oil by decanting.

(b) Alkaline Treatment

A100 mL of the degummed oils was separately placed in a beaker and agitated on a hot plate for about 5 minutes. 15 mL of 2.5 M NaOH (aq) solution was added to the beaker and stirred for 30 minutes. A thick mixture formed at the bottom of the beaker, which was believed to contain a mixture of soaps and the remaining phospholipids, was separated by decanting.

(c) Bleaching Treatment

A 100 mL of the neutralized oils was measured and placed in a beaker. The oils were heated to about 100 ºC to completely remove all water molecules present. A 0.1 g of activated charcoal was added, and the mixtures were heated for up to 45 minutes with constant stirring. The obtained mixture was centrifuged for 15 minutes at 2500 rpm using a C5 bench-top centrifuge**.**

Synthesis of Blend Oil Triester (BOTE)

(a) Synthesis of Blend Oil Methyl Ester (BOME) from BO

The refined peanut oil, soybean oil, and fish oil were mixed in a ratio of 1:1:2, respectively, using a magnetic stirrer for 30 minutes to create a homogeneous mixture (BO) and measured using ASTM standards (Abdelrahman *et al.,* 2017).

A known amount of BO was weighed and placed on a hot plate in a three-neck round-bottom flask equipped with a magnetic stirrer, refluxing condenser and a thermometer. A mixture of potassium hydroxide and methanol was added (a 1:6 BO to methanol ratio was used). The mixture was heated and stirred for 90 minutes at 60-65 °C. The product settled overnight and the top phase (crude ester) was separated from the bottom phase (glycerol) and washed three times with warm water to remove excess catalyst. The ester (BOME) was dried at 100 °C for 30 minutes and obtained (Mustapha *et al.,* 2023).

The N_M and percentage yield of BOME were calculated using the equations:

$$N_M = \frac{M_O \times MM_m \times R_m}{MM_o \times R_o}, \qquad (3)$$

$$\%Y = \frac{\text{weight of BOME produced}}{\text{weight of the oil sample used}} \times 100 \qquad (4)$$

where %Y is the Percentage yield, N_M is the amount of methanol, MM_o is the molecular weight of oil, MM_m is the molecular weight of methanol, M_o is the mass of oil, R_m and R_o are the ratios of methanol to oil sample.

(b) Synthesis of BOTE from BOME

A precise amount of BOME was measured into a 500 mL three-neck round-bottom flask and placed on a hot plate equipped with a magnetic stirrer, condenser, and thermometer. A mixture of potassium methoxide was prepared from potassium hydroxide and methanol, following a modified experimental procedure described by De Oliveira *et al.* (2011). The methoxide form was obtained after adding 8 g of KOH to 100 mL of methanol under stirring until complete dissolution (exothermic reaction). The methoxide was added as a catalyst, followed by TMP and the reaction was allowed to complete. The reaction was carried out with varying molar ratios of BOME to TMP, temperature (60-100 ˚C), and reaction time (60-120 min).

The amount of TMP used and the percentage yield of BOTE were calculated using the equations:

$$M_T = \frac{M_O \times MM_T \times R_T}{MM_0 \times R_0}, \qquad (5)$$

$$\%Y = \frac{\text{weight of Triester produced}}{\text{weight of Methyl ester used}} \times 100 \qquad (6)$$

where %Y is the Percentage yield, M_T denotes the mass of TMP, MM_o represents the molecular weight of BOME, MM_m is the molecular weight of methanol, M_o is the mass of BME, R_T and R_o are the ratio of TMP to BOME.

Design of Experiments (DOE)

RSM uses a Design of Experiments (DOE) with minimal data to create accurate analysis of variance (ANOVA) models. BBD was used due to its lack of axial points and requiring fewer experimental runs (Shaba *et al*., 2018). 17 experiments were conducted to explore the effect of three variables on triester yield (Table 2). The triester yield was calculated and incorporated into the BBD model for further analysis. The variables were evaluated on a scale of high (+), low (-), and medium (0). Five center points were used to estimate pure error and lack of fit for the suggested model, and a second-order polynomial equation was used to express triester synthesis as a function of the independent variables (Shaba *et al*., 2018):

$$Y = \beta_0 + \sum_{i=1}^{p} \beta_i X_i + \sum_{i=1}^{p} \beta_{ii} X^2 + \sum_{1 \le i \le j}^{p} \beta_{ij} X_i X_j + \varepsilon$$

, (7)

where Y, j, i, ε, p, β_i, and β_0 signify response factor, quadratic coefficient, linear coefficient, random number, number of factors, first-order model coefficient, and intercept. Multiple regressions were employed to fit the coefficients of the second-order polynomial models of the responses and were evaluated using ANOVA and tests of significance.

Validation of Result

In order to verify the result from the BBD model, experiments were conducted under the predicted conditions. The experimental and predicted percentage yield were compared and agree if their difference is <0.05 (Ejike *et al.,* 2021).

Lubricating Properties of BOTE

The synthesized BOTE lubricating properties, such as viscosity index, pour point, and flash point, were carried out using American Society for Testing and Materials-ASTM Standards.

(a) Pour Point

An oil sample (50 mL) was immersed in a cold-water bath and allowed to stand until it lost its flow features. The thermometer was used to measure the temperature at which the hazy appearance is shown.

(b) Flash Point

An oil sample (50 mL) was transferred into a crucible while the temperature of the oil sample was gradually raised. A thermometer was suspended into the sample to monitor its temperature rise, and the temperature at which the sample begins flashing but not supporting burning was noted as the flash point.

(c) Viscosity Index

The oil sample was poured into a test tube. After which, a spindle of 1 mm was attached to the viscometer and then inserted into the sample until the marked point on the spindle, making sure the spindle was not touching the container vessel. The experiment was run at specific times in triplicate at a speed rate of 30 rpm and at 40 and 100 ˚C.

According to ASTM D2270, viscosity index is determined by comparing the viscosity of the oil with viscosity of two reference oils L and H at constant temperature.

The viscosity index was determined using the equation:

$$(VI) - \frac{L - U}{L - H} \times 100, \qquad (8)$$

Where VI is Viscosity Index, U is the kinematic viscosity of sample at 40 ˚C, L is the kinematic viscosity at 40 ˚C of an oil of zero (0) viscosity index having the same kinematic viscosity at 100 ˚C as sample and H is the kinematic viscosity at 100 ˚C of an oil of 100 viscosity indexes having the same kinematic viscosity at 100 ˚C as sample.

Results and Discussion

Lubricating Properties of BOTE

BOTE was subjected to specific property tests to ascertain its applicability as a lubricating oil using the ASTM standard methods. These properties include flash point (FP), pour point (PP), and viscosity index (VI), and are shown in Table 1.

The fluidity of a lubricant at low temperatures is crucial, which is determined by its pour point (PP). The PP is the minimum temperature at which the biolubricant oil will pour or flow when it is cooled. The PP should be low enough to ensure that the biolubricant is pumpable when the equipment is initiated at extremely low temperatures. In this study, a PP value of -2.5 ˚C was obtained, and this value closely matches the ISO VG 32 standard of -6 ˚C for gear oil temperature limits. This is similar to the value (-6) reported by Mustapha *et al*. (2023). Hence, the synthesized BOTE has excellent cold flow properties.

To evaluate a lubricant's flammability, one looks at its flash point. Flash point (FP) is the lowest temperature at which a biolubricant will form a vapour in the air near its surface that will briefly ignite on exposure to an open flame. The FP should be high to allow safe operation and minimum volatilization at the maximum operating temperature. The FP value of BOTE was found to be 205 °C and this value matches the ISO standard of above 204 and is close to the findings in literature; for example, an FP of 215 and 210 °C was documented by Ifeanyi-Nze and Akhiehiero (2023) and Mustapha *et al*. (2023) for *Jatropha* biolubricant and sweet almond biolubricant, respectively. Thus, it is considerably high enough to be used for lubrication.

The viscosity index (VI) is an arbitrary numbering scale that indicates the changes in oil viscosity with temperature changes. That is, the VI highlights how the biolubricant viscosity changes with the temperature variation. If the VI is low, the viscosity's temperature dependence is high, while a high VI indicates that the viscosity changes little across a broad temperature range. More precisely, a higher VI indicates a better-quality lubricant. BOTE showed a high VI of 136 calculated from the viscosity values recorded at 40 °C and 100 °C to be 72.7 and 11.8 mPa/s, respectively. It can be classified as a high-VI fluid-based ester that matches the ISO VG-32 standard requirements and is suitable for use in a wide range of engines. High VI values have been reported by several researchers, especially values greater than 90. For instance, Ifeanyi-Nze and Akhiehiero (2023), Mustapha *et al*. (2023), and Jumaah *et al*. (2022) reported a high VI value of 205, 130, and 141 to 187 ˚C, respectively.

Optimization of Reaction Conditions for BOTE Synthesis

The experimental data from 17 experiments under BBD's suggested reaction conditions were used to develop a model (Table 2). It was inferred that the percentage triester yield was between 83.42 – 90.95 %, with a maximum percentage yield of 90.95 %. This is in line with the findings of Ifeanyi-Nze and Akhiehiero (2023), having percentage yields of 94.12 % respectively, although at different reaction conditions.

3.2.1 BBD Model fitting

The BBD model was used to evaluate various models, including linear, two-factor interaction (2FI), quadratic, and cubic models, to determine the best fit for experimental data (Table 3). The quadratic model was recommended as the best fit due to its significant coefficient of determination (R^2 value). Linear and 2FI models were eliminated due to their failure to forecast answers. The cubic model was not chosen due to its "alias" status, indicating the need for more tests to estimate all model terms independently.

Also, the adjusted R^2, lack of fit, predicted R^2, and sequential p-value for the observed data are 0.9762, 0.3527, 0.9054, and 0.0010, respectively. A p-value less than 0.05 indicates the model's significance with a 95 % confidence interval. To be appropriate, the lack of fit should be non-significant, as it assesses between pure and residual errors (Shaba *et al.,* 2018). Thus, a non-significant lack of fit is expected for this study. Furthermore, a high R^2 value of 0.9896 and a low C.V.% % of 0.3358 were seen. This only indicates that the model satisfactorily represents the relationship between the independent variables (molar ratio, temperature, and reaction time) and the response (triester yield) and that the experiment is reliable and precise. The predicted R^2 value of 0.9054 is in reasonable agreement with the adjusted R^2 value of 0.9762, i.e., the difference is less than 0.2. Adequate precision measures the signal-to-noise ratio. A ratio greater than 4 is desirable. A ratio of 32.833 achieved in this study indicates an adequate signal. This confirms that the quadratic model can be used to adequately navigate the design space.

Table 1: Lubricating properties of BOTE

Lubrication Properties	**BOTE**	**JBL[a]**	**SAL[b]**	**ISO Viscosity Grade**	**BOTE**	**JBL[a]**
				46	**32**	**68**
Viscosity @ 40 ˚C (mPa/s)	72.7	61.08	42.1	≥ 41.4	72.7	61.08
Viscosity @ 100 ˚C (mPa/s)	11.8	9.21	8.9	> 4.1	11.8	9.21
Viscosity Index (ASTM 227O)	136	205	198.79	≥ 90	136	205
Pour Point (˚c)	- 2.5	- 15	- 6	-10	- 2.5	- 15
Flash Point (˚c)	205	215	210	220	204	250

Key: JBL[a]: Jatropha Biolubricant (Ifeanyi-nze and Akhiehiero, 2023)
SAL[b]: Sweet Almond Lubricant (Mustapha et al., 2023)

ANOVA of Percentage Triester Yield

The experimental design of triester synthesis involved three reaction conditions (molar ratio, temperature, and reaction time) and the combined effects of these conditions were examined. The quadratic polynomial equation proposed by BBD was found to be the most suitable regression equation for estimating triester percentage yield, and a second-order equation was suggested.

The final equation in terms of coded factors is presented below:

$$Y = +85.52 + 0.8288\,A - 2.06\,B + 0.0425\,C - 1.5\,AB - 0.2275\,AC + 0.6025\,BC + 0.6420\,A^2 + 0.0.1420\,B^2 + 0.7795\,C^2$$

(9)

where Y, A, B, and C stand for triester yield (%), molar ratio (wt%), temperature (°C), and reaction time (min), respectively. Also, AB, AC, and BC, represent the linear interaction effects between two variables, and A^2, B^2 and C^2 depict the quadratic impacts of the independent variables. The equation in terms of coded factors can be used to make predictions about the response at given levels of each factor, with high levels coded as +1 and low levels as -1.

Table 2: Percentage Yield of Synthesized BOTE Using the Experimental Design

Std	Runs	A: Molar Ratio (wt. %)	B: Temperature (˚C)	C: Reaction Time (Min)	Actual Yield (%)	Predicted Yield (%)
13	1	5	80	90	85.17	85.52
9	2	5	60	60	89.08	89.05
7	3	3	80	120	86.58	86.38
16	4	5	80	90	85.33	85.52
4	**5**	**7**	**100**	**90**	**83.42**	**83.48**
3	6	3	100	90	84.83	85.01
1	7	3	60	90	86	85.94
6	8	7	80	60	87.75	87.95
12	9	5	100	120	85	85.03
14	10	5	80	90	85.58	85.52
15	11	5	80	90	85.67	85.52
11	12	5	60	120	87.67	87.93
17	13	5	80	90	85.83	85.52
8	14	7	80	120	87.67	87.58
5	15	3	80	60	85.75	85.84
10	16	5	100	60	84	83.74
2	**17**	**7**	**60**	**90**	**90.95**	**90.77**

Table 3: Lack of fit test and Fit summary

Source	Sum of Squares	df	Mean Square	Seq. p-value	Lack of Fit p-value	Adj. R²	Pred. R²	Remarks
Linear	16.81	9	1.87	0.0011	0.0032	0.6272	0.4170	
2FI	5.04	6	0.8402	0.0068	0.0155	0.8491	0.7277	
Quadratic	**0.3063**	**3**	**0.1021**	**0.0010**	**0.3527**	**0.9762**	**0.9054**	**Suggested**
Cubic	0.0000	0	-	0.3527	-	0.9801	-	**Aliased**

The coded equation is useful for identifying the relative impact of the factors by comparing the factor coefficients. The ANOVA analysis of a quadratic model for triester synthesis was analyzed using the F test to establish its statistical significance, as presented in Table 4. The results showed that A, B, AB, BC, A^2, and C^2 were significant, having p-values <0.05 and temperature (B) had the most significant influence on triester yield, with an F-value of 403.34. The F-value represents the significance of the effect of a given independent parameter on a dependent variable (Ifeanyi-Nze & Akhiehiero, 2023). The model F-value of 73.98 indicates that the model is significant, with a 0.01 % chance of it occurring due to noise. The F-value of 1.45 indicates that the Lack of Fit is not significant relative to the pure error, with a 35.27 % chance of it occurring due to noise.

Table 4: ANOVA for Quadratic Model of Triester Synthesis

Source	Sum of Squares	df	Mean Square	F-value	p-value	Remark
Model	**55.8400**	**9**	**6.2000**	**73.9800**	**< 0.0001**	**Significant**
A-Molar Ratio	5.4900	1	5.4900	65.5200	< 0.0001	
B-Temperature	33.8300	1	33.8300	403.3400	< 0.0001	
C-Reaction Time	0.0144	1	0.0144	0.1723	0.6905	
AB	10.1100	1	10.1100	120.5800	< 0.0001	
AC	0.2070	1	0.2070	2.4700	0.1601	
BC	1.4500	1	1.4500	17.3100	0.0042	
A^2	1.7400	1	1.7400	20.6900	0.0026	
B^2	0.0849	1	0.0849	1.0100	0.3478	
C^2	2.5600	1	2.5600	30.5100	0.0009	
Residual	0.5870	7	0.0839			
Lack of Fit	**0.3063**	**3**	**0.1021**	**1.4500**	**0.3527**	**Not significant**
Pure Error	0.2807	4	0.0702			
Cor Total	56.4300	16				

*Factor coding is **coded**. The sum of squares is **Type III – Partial**.*

Model prediction

The similarities between the actual and predicted responses obtained are shown in Table 5. The quadratic model showed a strong statistical correlation between the actual and predicted responses, as indicated by the close correlation coefficients (R^2) of 0.9054 and 0.9762, indicating excellent predictive capability (Mustapha *et al.,* 2020). The difference between the predicted and adjusted R^2 is 0.0708, indicating reasonable agreement. Residuals are crucial for identifying.

Outliers and quantifying residues concerning the standard deviation of experimental data. The residual value is the difference between the predicted and actual response values.

The normal plot of residuals and the predicted vs. actual plot are presented in Figures 1a and 1b, respectively, and were utilized to assess if data points form a straight line. A non-linear pattern indicates non-normality in the error term, which can be resolved by a transformation. The residual points align closely on the normal plot, indicating the model's accuracy (Figure 1a). Furthermore, Figure 1b shows a close distribution of data points between the actual and predicted percentage triester yield, demonstrating an excellent correlation between these values, confirming the model's ability to adequately predict the response variable in actual values.

Table 5: Report on the Actual and Predicted Value of Triester Synthesis

Standard Order	Run Order	Actual Value	Predicted Value	Residual	Internally Studentized Residuals	Externally Studentized Residuals
13	1	85.17	85.52	-0.3460	-1.336	-1.433
9	2	89.08	89.05	0.0263	0.181	0.168
7	3	86.58	86.38	0.2012	1.390	1.512
16	4	85.33	85.52	-0.1860	-0.718	-0.691
4	5	83.42	83.48	-0.0625	-0.432	-0.405
3	6	84.83	85.01	-0.1750	-1.209	-1.258
1	7	86.00	85.94	0.0625	0.432	0.405
6	8	87.75	87.95	-0.2013	-1.390	-1.512
12	9	85.00	85.03	-0.0263	-0.181	-0.168
14	10	85.58	85.52	0.0640	0.247	0.230
15	11	85.67	85.52	0.1540	0.595	0.565
11	12	87.67	87.93	-0.2638	-1.822	-2.325
17	13	85.83	85.52	0.3140	1.212	1.263
8	14	87.67	87.58	0.0888	0.613	0.583
5	15	85.75	85.84	-0.0887	-0.613	-0.583
10	16	84.00	83.74	0.2637	1.822	2.325
2	17	90.95	90.77	0.1750	1.209	1.258

Key: *(1) Exceeds limits. Current Transform:* ***Yield****. Recommended Transform:* ***None***

Effect of Input Variables on Percentage Triester Yield

The ANOVA analysis only determined the impact of an input variable on the response, but did not explain the effect of the variables on the response and their interactions. To investigate this, three-dimensional (3D) and two-dimensional (2D) response surface plots were used.

(a) Effect of One Input Variable

The response surface plot for the effect of molar ratio of BOME to TMP (A), temperature (B), and reaction time (C) is as shown in Figure 2a, 2b, and 2c, respectively. It was demonstrated that an increase in A increases the percentage yield of triester synthesis. Hence, the highest triester yield was obtained at the highest A. It was also observed that as B decreases, the percentage of triester synthesis increases. Thus, the optimum yield was achieved at low B. Furthermore, the reaction time (C) affects the triester yield, and this effect is not unidirectional, with increasing C causing a decrease in yield until a point where further increase in

C increases yield. Therefore, the highest percentage triester yield was achieved at the lowest or highest C.

(b) Effect of Two Input Variables

The 2D and 3D response surface plot for the combined impact of the molar ratio of BOME to TMP and temperature (AB), molar ratio of BOME to TMP and reaction time (AC), and temperature and reaction time (BC), on percentage triester yield is shown in Figure 3a, 3b, and 3c respectively. The effect of AB was examined while keeping C constant at 90 min, and it was deduced that high triester yield was achieved at high A and low B (Figure 3a). Also, the effect of AC was investigated at a constant B of 80 ˚C, and it was revealed that a high triester yield could be obtained at a high A with a low or high C. At the beginning of the reaction, increasing A increases the percentage triester yield but decreases as the reaction progresses, until a point is reached where further increases lead to an increase in triester yield (Figure 3b). Subsequently, the effect of BC was conducted at a fixed A of 5:1, and it was observed that, optimum percentage triester yield was realized at a low B and a low C (Figure 3c). However, increase in temperature over time is expected to increase the triester yield due to its ability to improve mass transfer rate and conversion but, at extreme temperatures and prolonged reaction times, the evaporation of BOME occurs, causing less of it to remain in the reaction vessel, leading to lower conversion (Gul *et al.,* 2021).

(c) Effect of Three Input Variables

The perturbation plot describes the variation in response when reaction parameters deviate from the reference point, while all other components remain constant (Ifeanyi-Nze & Akhiehiero, 2023). The perturbation plot for three input variables before and after optimization, as seen in Figure 4, shows that all three variables significantly affect the percentage triester yield, although B has a negative effect.

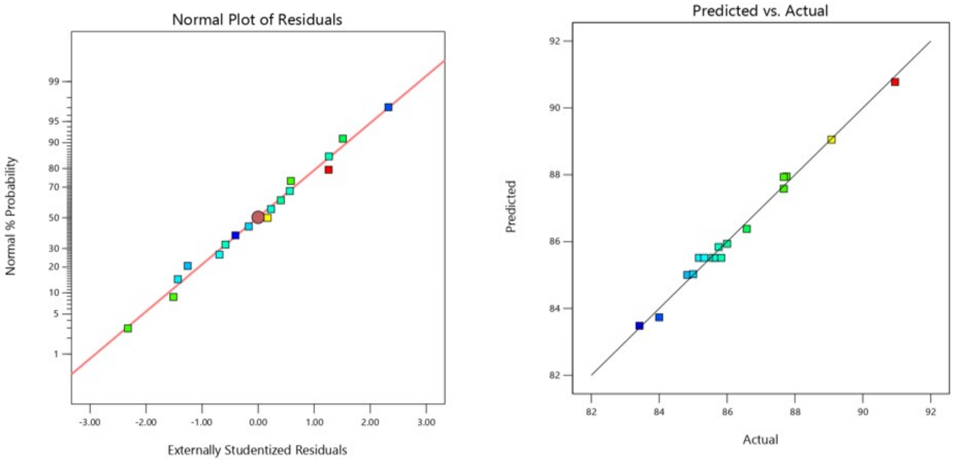

(a) **(b)**

Figure 1: (a) Normal Plot of Residuals (b) Predicted vs Actual for Triester Synthesis

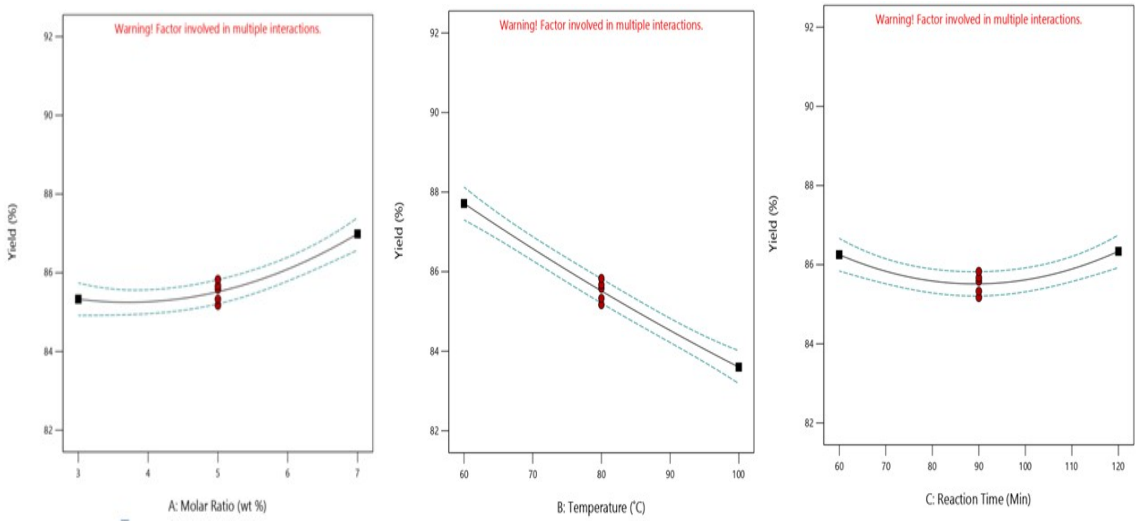

Figure 2: Effect of one variable [(a) A (b) B (c) C] on Percentage Triester Yield

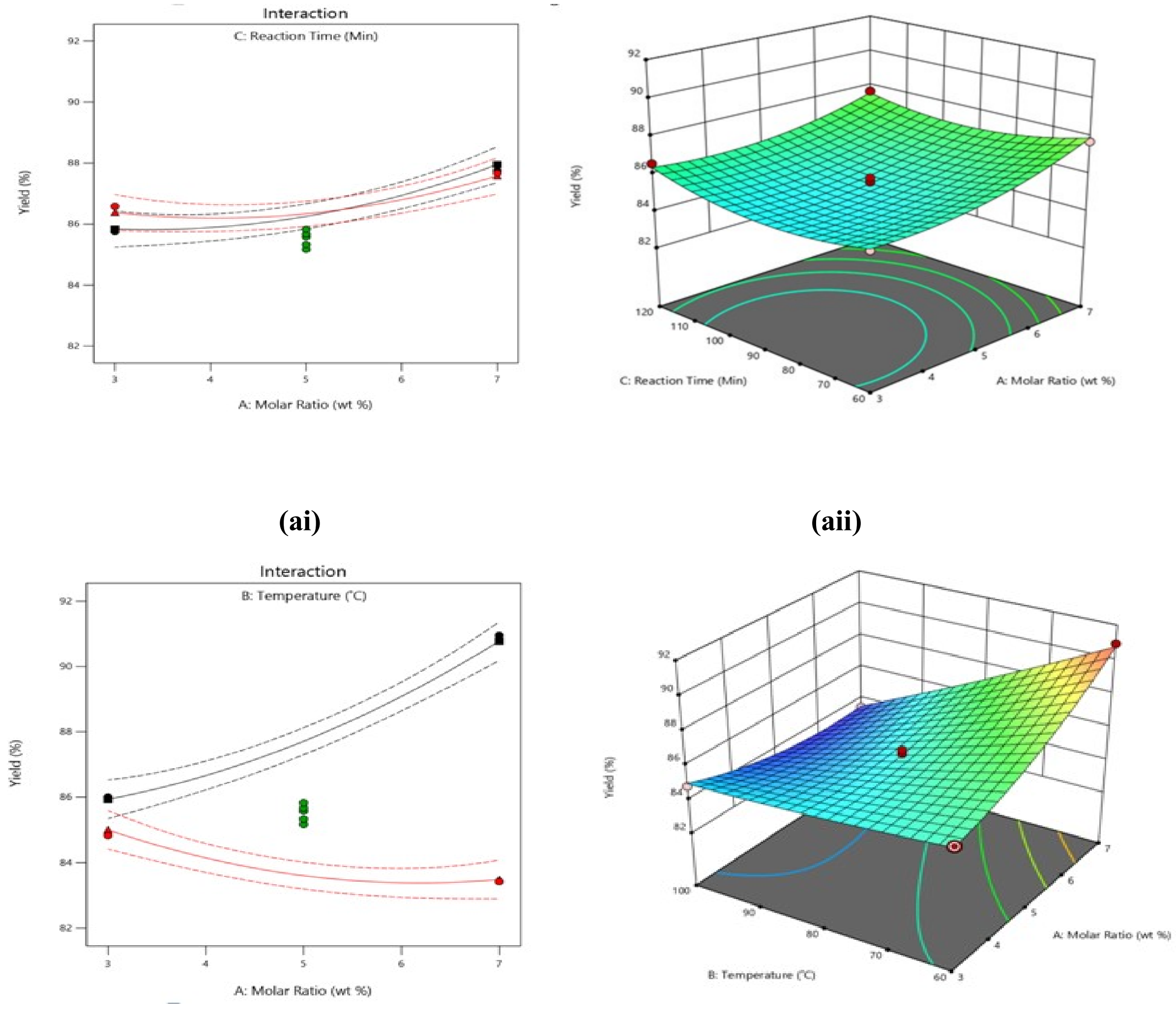

(ai) **(aii)**

(bi) **(bii)**

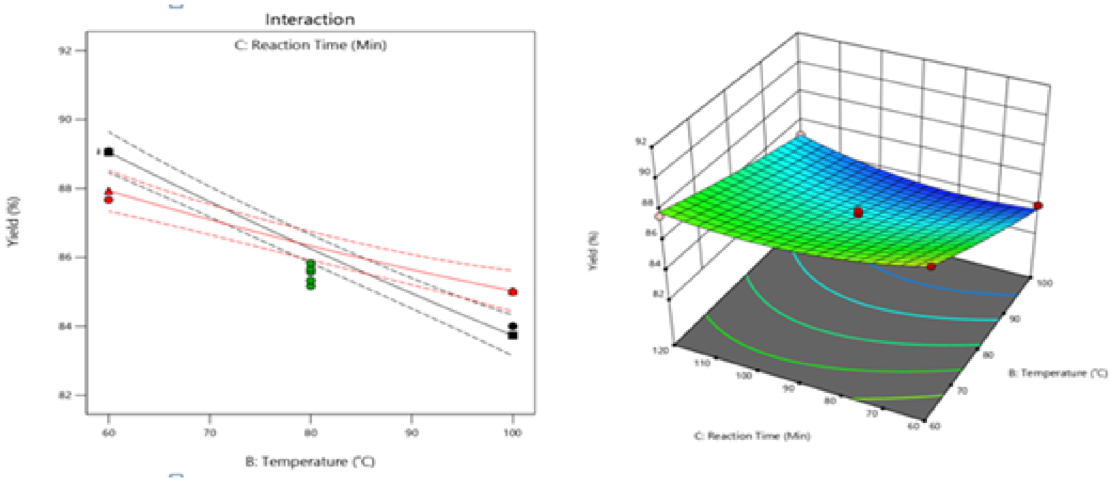

(ci) **(cii)**

Figure 3: (i) 2D and (ii) 3D Response Surface Plots for Effect of Two Variables [(a) AB (b) AC (c) BC] on Percentage Triester Yield.

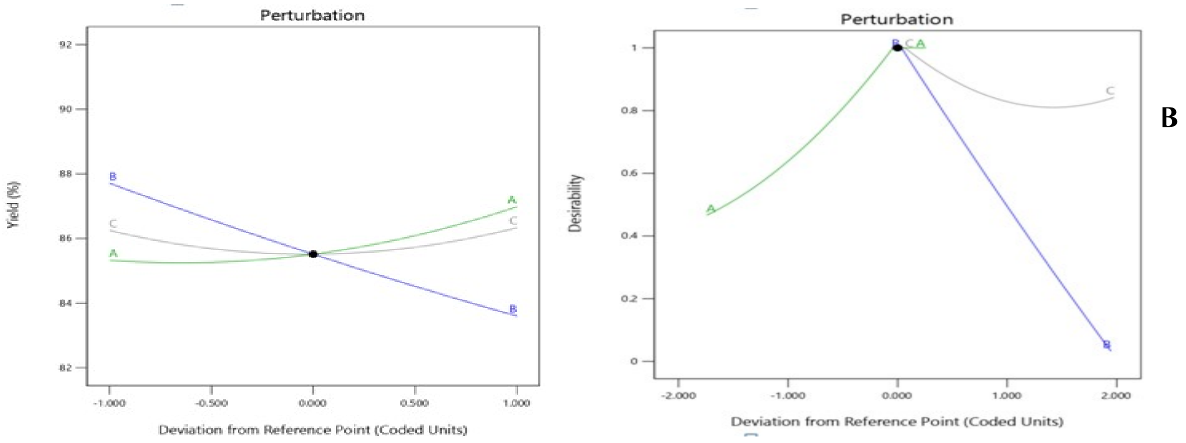

(a) **(b)**

Figure 4: Perturbation Plots for Effect of Three Variables (a) before and (b) After Optimization.

3.2.5 Process Variable Optimization

This study used Design-Expert 13 software to solve a regression equation to determine the best conditions for input variables. The software employed numerical optimization techniques based on desirability function and point prediction to predict triester yield. The software predicted multiple input variables for maximum percentage triester yield and suggested the first optimal conditions of A of 6.5:1, B of 61.1 ˚C, C of 60.8 min, and a percentage yield of 91.097 % with 1.0 desirability value (Table 6).

Table 6: Optimization Result for the Optimum Process Variables

S/N	Molar Ratio	Temperature	Reaction Time	Yield (%)	Desirability	Remark
1	**6.484**	**61.061**	**60.751**	**91.097**	**1.000**	**Selected**
2	6.896	60.985	61.296	91.822	1.000	
3	6.910	61.770	63.175	91.541	1.000	
4	6.997	60.068	83.201	90.974	1.000	
5	6.984	60.086	82.755	90.963	1.000	
6	6.988	62.270	73.270	90.953	1.000	
7	6.949	60.633	72.329	91.278	1.000	
8	6.999	60.147	81.297	91.036	1.000	
9	6.756	61.377	67.714	91.040	1.000	
10	6.923	60.732	76.912	90.971	1.000	

Validation of Optimized Process Variables

A triplicate confirmatory experiment was conducted to verify the accuracy, applicability, and reproducibility of predicted results. The mean triester yield was found to be 90.967 %, within the model's predicted range. This excellent agreement with the experimental mean value of 90.977 % and predicted value of 91.097 % with a percentage error of <5 %, validates the predicted optimum conditions, indicating that BBD is an effective tool for optimizing this process.

Conclusion and Recommendation

This study demonstrated the synthesis of a low-cost biolubricant through the transesterification of blend oil methyl esters (obtained from a blend of crude and waste cooking oils) with TMP using potassium methoxide as a catalyst. Also, BBD-based RSM efficiently optimized the reaction conditions, including the BOME to TMP molar ratio (3:1–7:1 wt%), temperature (60–100 ˚C), and reaction time (60–120 min) to obtain a high triester yield. Subsequently, the ANOVA and model fittings showed that the quadratic regression polynomial model was effective for this process, with variables A (molar ratio) and B (temperature) having a more significant effect. Similarly, the optimum triester yield of 91.097 % was achieved at a molar ratio of BOME to TMP of 6.5:1, a temperature of 61.1 ˚C, a reaction time of 60.8 min, and a desirability value of 1.0. At these predicted optimum conditions, an experimental mean value of 90.977 % yield was achieved, and the synthesized biolubricant was found to meet the ISO VG 32 standard. This was found to be in excellent agreement with the predicted value. Further research is needed to develop better quality biolubricant using one or a combination of other chemical modifications. Also, optimization of reaction conditions using other RSM designs, such as central composite design (CCD) and Doehlert design, should be investigated.

Acknowledgements

The authors express their sincere gratitude to the Department of Chemistry and Industrial Chemistry, Faculty of Pure and

Applied Sciences, Kwara State University, Malete, Nigeria, for their significant research.

References

Abdelrahman, B. F., Emaad, T. B. A., & Mohammed, A. A. (2017). Biodiesel Production from Mixed Non-Edible Oils, Castor Seed Oil and Waste Fish Oil. *Fuel*, 210, 721-728. http://dx.doi.org/10.1016/j.fuel.2017.09.009.

Alang, M. B., Ndi-kontar, M. K., Sani, Y. M., & Ndifon, P. T. (2018). Synthesis and Characterization of a Biolubricant from Cameroon Palm Kernel Seed Oil Using a Locally Produced Base Catalyst from Plantain Peelings. *Green and Sustainable Chemistry*, 8, 275-287. https://doi.org/10.4236/gsc.2018.83018

Appiah, G., Tulashie, S. K., Akpari, E. E. A., Rene, E. R., & Dodoo, D. (2021). Biolubricant production via esterification and transesterification processes: Current updates and perspectives. *International Journal of Energy Research,* 1-32. DOI: 10.1002/er.7453

Bashiri, S., Ghobadian, B., Dehghani, S. M., & Gorjian, S. (2021). Chemical Modification of Sunflower Waste Cooking Oil for Biolubricant Production through Epoxidation Reaction. *Materials Science for Energy Technologies,* 4, 119-127. doi:10.1016/j.mset.2021.

Betiku, E., Akintunde, A. M., & Ojumu, T. V. (2016). Banana Peels as a Biobase Catalyst for Fattyacid Methyl Esters Production Using Napoleon's Plume (*Bauhinia monandra*) Seed Oil: A Process Parameters Optimization Study. *Energy*, 103, 797-806. https://doi.org/10.1016/j.energy.2016.02.138.

Chaiendoo, K., Ob-Eye, J., & Itthibenchapong, V. (2025). Preparation and physicochemical properties of a new biolubricant from epoxidized fatty acids and diethylene glycol monomethyl ether. *ACS Omega*, *10*(18), 19010–19018. https://doi.org/10.1021/acsomega.5c01223.

De Oliveira, M. F., Vieira, A. T., Batista, A. C. F., Rodrigues, H. S., & Stradiotto, N. R. (2011). A simple and fast method for the production and characterization of methylic and ethylic biodiesels from tucum oil via an alkaline route. *Journal of Biomedicine and Biotechnology,* 2011:1-4. https://doi.org/10.1155/2011/238474.

Ejike, E. O., Stone, R. O., & Okechukwu, D. O. (2021). The Synthesis and Optimization of A Trimethylolpropane Based Biolubricant from a Lard Oil Base Stock. *The Pharmaceutical and Chemical Journal,* 8(5), 1-11

Gul, M., Zulkifli, N. W. M., Kalam, M. A., Masjuki, H. H., Mujtaba, M. A., Yousuf, S., Bashir, M. N., Ahmed, W., Yusoff, M. N. A. M., Shazia, N., & Rauf A. (2021). RSM and Artificial Neural Networking based production optimization of sustainable Cotton bio-lubricant and evaluation of its lubricity & tribological properties. *Energy Reports,* 7, 830–839. https://doi.org/10.1016/j.egyr.2021.01.033.

Ifeanyi-nze, F. O., & Akhiehiero, E. T. (2023). Optimization of the process variables on biodegradable industrial lubricant basestock synthesis from Jatropha curcas seed oil via response surface methodology. *Frontiers in Energy Research*, 11, 1–15.

https://doi.org/10.3389/fenrg.2023.1169565

Jumaah, A., Salih, N., & Salimon, J. (2022). D-Optimal Design Optimization for Esterification of Palm Fatty Acids Distillate with Polyhydric Alcohols for Biolubricants Production. *Iran. J. Chem. Chem. Eng.,* 41(5), 1657-1672.

Mustapha, A. O., Adepoju, R. A., & Afolabi, Y. T. (2020). Optimization of Vegetable Oil-Based Biodiesels by Multi-Response Surface Methodology (MRS) using Desirability Functions. *Journal of Chemical Society of Nigeria*, 45(5), 917–924.

Mustapha, A. O., Adepoju, R. A., Ajiboye, R. Y., Afolabi, Y. T., Jimoh, A. A., & Abdulsalam, Z. A. (2021). Production, properties and fatty acids profile of some refined vegetable oils-based biodiesels. *Asian Journal of Advances in Research*, 17–26.

Mustapha, A. O., Babatunde, A., Akinola, O., Olododo, H. S., Afolabi, Y. T., & Abdulfatai, T. (2023). Trimethylolpropane-based Biolubricant Synthesis from Sweet Almond (*Prunus amygdalus dulcis*) Seed Oil for Use in Automotive Applications. *Journal of Turkish Chemical Society A: Chemistry,* 10(2), 371-380.

Nkem, C. S., & Nwakaudu, M. S. (2019). Process Optimization and Modelling of Lubricant Base Stock Synthesis from Crude Palm Oil. *International Journal of Research and Innovation in Applied Science,* 4(5), 2454-6194.

Ocholi, O., Menkiti, M., Auta, M., & Ezemagu, I. (2018). Optimization of the operating parameters for the extractive synthesis of biolubricant from sesame seed oil via response surface methodology. *Egyptian Journal of Petroleum*, *27*(3), 265–275. https://doi.org/10.1016/j.ejpe.2017.04.001

Raof, N. A., Hamid, H. A., Mohamad-Aziz, N. A., & Yunus, R. (2022). Prospects of Plant-Based Trimethylolpropane Esters in the Biolubricant Formulation for Various Applications: A Review. *Frontiers of Mechanical Engineering*, 8, 1-21.

Shaba, M. I., Mohammed, A., Musa, D. S., Audu, B. A., & Katamba, Y. B. (2018). Synthesis and Optimization Process of Ethylene Glycol-Based Bio-lubricant Synthesis and Optimization Process of Ethylene Glycol-Based Bio - lubricant from Palm Kernel Oil (PKO). *Journal of Renewable Energy and Environment*, 5(2), 1-9

Soufi, M. D., Ghobadian, B., Mousavi, S. M., Najafi, G., & Aubin, J. (2019). Valorization of Waste Cooking Oil Based Biodiesel for Biolubricant Production in a Vertical Pulsed Column: Energy Efficient Process Approach. *Energy*, 189. doi:10.1016/j.energy. 2019.116266.

Thanaphorn, R., Nisa, P., Tewan, Y., Sappasith, K., & Kanokphorn, S. (2018). Synthesis and Characterization of Biolubricant from POME Oil and Hepatopancreas Lipase from Pacific White Shrimp (*Litopenaeus vannamei), Chiang Mai Journal of Science,* 45(6): 2438-2453.

Zayyanu, I., Saidu, R. S., Mohammed, M. L., Almustapha, N. M., & Sadiq, M. E. (2025). Production And Process Optimization of Biolubricant from Neem Seed Oil. *International Journal Of Science For Global Sustainability (A Publication of Faculty of Science, Federal University Gusau, Nigeria),* 10 (1):2488-9229. doi.org/10.57233/ijsgs.v10i1.602.